Spatial and Spectral Optimization of Two-photon Imaging Data for Label-free Texture-based Tissue Classification Models

Thomas G. Knapp[1], Suzann Duan[2], Juanita L. Merchant[2], Travis W. Sawyer[1,2,3]

Department of Biomedical Engineering,[1] College of Medicine,[2] and College of Optical Sciences,[3] University of Arizona

Biomedical Optics & Optical Measurement

THE UNIVERSITY OF ARIZONA

Background and Aim(s)

Duodenal gastrinoma (DGAST) neoplasms are commonly diagnosed at a late stage due to their characteristically small size and slow growth. Their tendency to grow diffusely in the duodenum [**Figure 1**] complicates surgical removal, increasing the chance of incomplete resection [1].

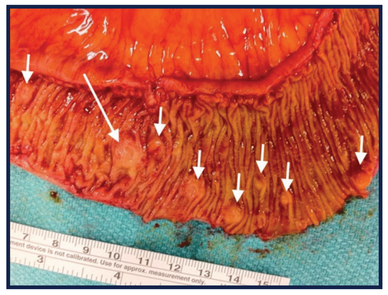

Figure 1:
Multi-focal neuroendocrine tumors (NETs) that have grown in the submucosa of the small bowel, indicated by the white arrows.
Current intraoperative imaging techniques are not capable of determining if these small tumors have been fully removed during surgical resection. Incomplete removal of tumors has been linked to decreased patient survival [2].
Resected samples are sent to pathology, where a lengthy process of examination is performed to determine if an adequate amount of healthy tissue surrounds the tumor, indicating that all cancer cells have been removed.
Surgical revision for incomplete removal is detrimental to patient well-being, necessitating a method for rapid assessment of tumor resection sites during the time of procedure.

We have investigated the use of multiphoton microscopy (MPM) to generate label-free images of human DGASTs. The high spatial resolution and imaging depth of MPM supports its incorporation as a margin analysis probe into a multimodal laparoscope [**Figure 2 A**]. MPM channels were tuned to collect signal from endogenous fluorophores with known spectra and links to cell pathways perturbed in cancer development [**Figure 2 B**]. Classifiers trained on MPM image texture features of formalin-fixed paraffin-embedded specimens discerned between images of normal and malignant tissue with a high degree of accuracy [**Figure 2 C**]. Acquisition of multiple channels is unfeasible for clinical use, requiring optimization of imaging parameters [**Figure 2 D**].

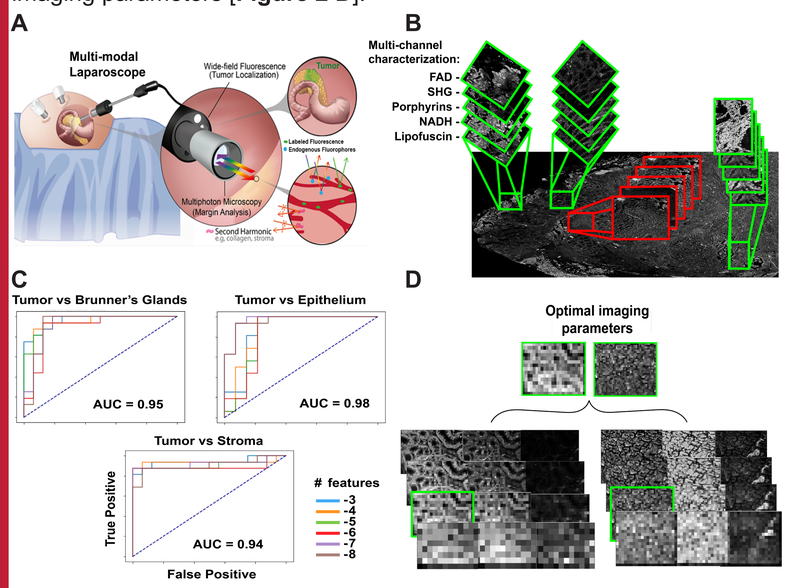

Figure 2: Depiction of the motivation for this work. (A) Illustration of a multi-modal laparascope with: 1. a wide-field fluorescence probe meant to detect labeled fluorescence for receptors highly expressed by DGASTs, and 2. a multi-photon microscopy (MPM) probe designed to use label-free contrast generated from tissue autofluorescence to identify normal and malignant cells. (B) The five autofluorescence channels and separate tissues of interest that were used to characterize the DGAST samples (normal tissue bounded in green, tumor bounded in red). (C) Receiver operating characteristic curves of linear-discriminant analysis image classifiers. Texture features were extracted from the MPM images and used to train these classifiers that correctly distinguished between images of tumor vs normal duodenal tissue with a high level of accuracy. (D) Determining which channels result in the greatest classification accuracy at varying levels of image resolution can help us predict the optimal paramters for the MPM probe that will be incorporated into the laprascope system. Doing so would significantly reduce acquisition time without sacrificing diagnostic power.

Methods

Images are first transformed into gray-level co-occurrence matrices (GLCM), which are generated for four pixel pair orientations and averaged due to the random orientation of tissue during in-vivo imaging leading to rotational independence. [**Figure 3 A**] Images were then down-sampled to reduce their spatial resolution [**Figure 3 B**], and texture feature extraction was repeated. Principal component analysis (PCA) was used to eliminate redundancy in the texture features prior to the training of linear discriminant analysis (LDA) classifiers. PCA-LDA classifier accuracy was measured using a leave-one-out approach with all possible combination of features within feature subsets ranging from 2 to 7 features. The original MPM features most correlated with the PC features resulting in the highest PCA-LDA classifier accuracy were then extracted for each degree of image down-sampling [**Figure 3 C**].

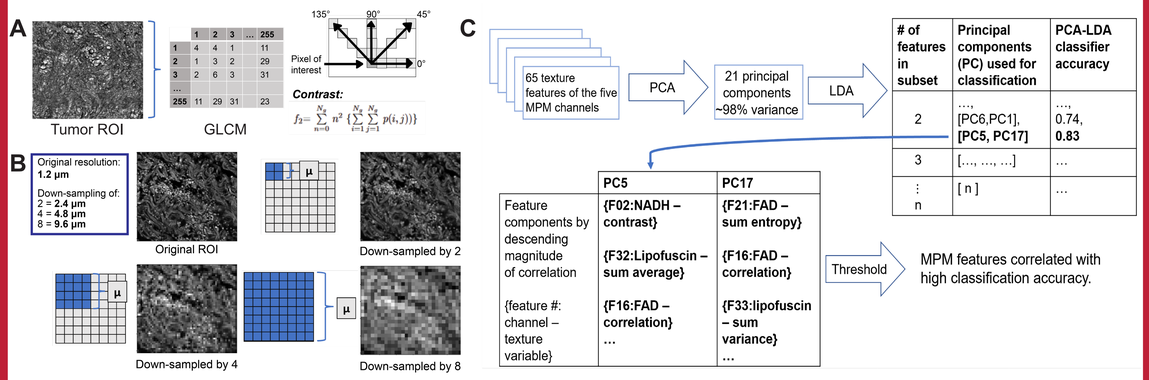

Figure 3: (A) Generation of a gray-level co-occurrence matrix from a DGAST multi-photon image. Each element of the GLCM is the frequency of pixels with intensity = [row, column] values being immediately adjacent, ex: element [3, 17] = # of pixels with intensity 3 next to pixels of intensity 17 in either the horizontal, vertical, or diagonal direction, depending on the GLCM. Shown is one of thirteen equations for image texture described by Haralick [3], contrast, where p(i,j) = (i,j)th entry in the GLCM and N_g = number of distinct gray levels in quantized image. (B) Process of down-sampling images, done through the averaging of pixels within n x n regions corresponding to the degree of downsampling to create pixels for the lower resolution images (C) Flow diagram of the process used to determine the optimal imaging channels and resolution. The threshold for features correlated to each principal component was a correlation greater than the standard deviation.

Results

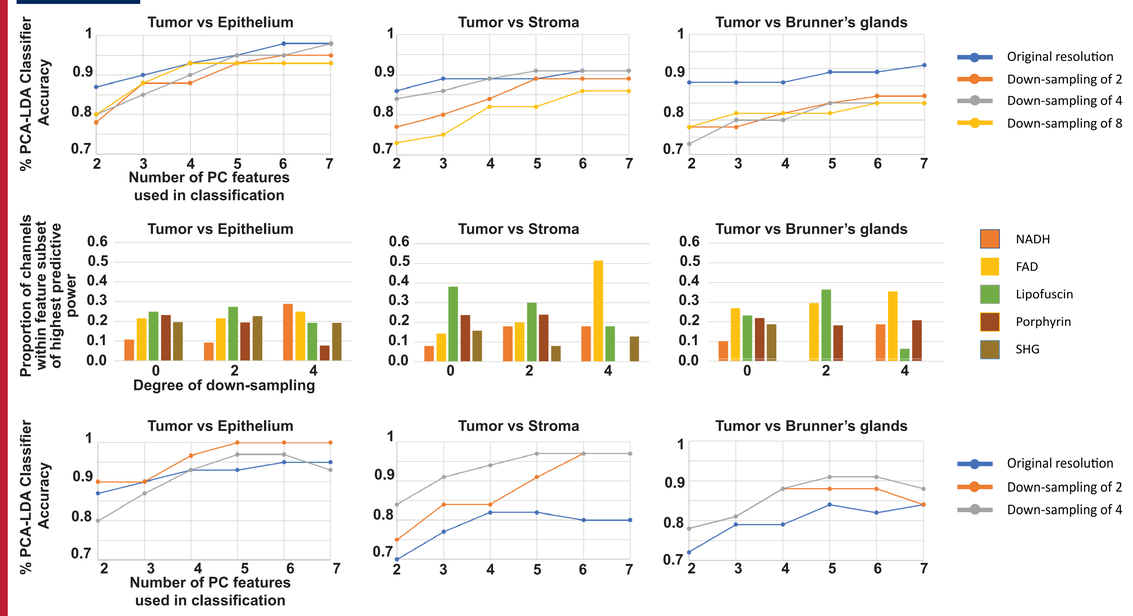

Figure 4: Top row - PCA-LDA classification accuracy in relation to degree of down-sampling. The drop in classification accuracy for the down-sampling of eight was great enough to remove it from subsequent analysis. Middle row - proportion of each channel used to achieve highest classification accuracy at different resolutions. In all but a single case, either the FAD or Lipofuscin channel were used in the greatest proportion. Bottom row - result of only using features from the FAD and LIpofuscin channels which show a marked improvement in classification accuracy at lower image resolutions.

Model Improvements

Several assumptions are being made with this model and it is limited by the initial acquisition being done using fixed tissue. The inclusion of image sampling and point spread function models [**Figure 5**] specific to the system of interest would improve the utility of the proposed methods for determining design parameters.

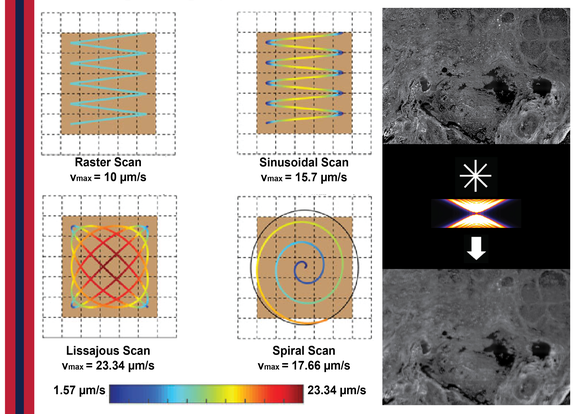

Figure 5: Models of various image sampling methods (adapted from Teo et al. [4]) (left) and an example of how a point spread function (PSF) would be incorporated into this model, i.e., by convolving the original high-resolution image data by a PSF model based on the system optics (right).

Conclusions

Texture features of label-free multi-photon microscopy images result in a high accuracy of classification between duodenal tissue types using linear discriminant analysis.
Classification accuracy is changed in basic models of lower image resolutions, suggesting boundaries of acceptable imaging parameters.
The improvement of classification accuracy with elimination of channel features based on this optimization process indicates potential utility for system design [**Figure 4**].

Acknowledgements

Special thanks to the Marley Imaging Core supervisor, Patty Jansma, for her assistance with the multi-photon microscope, and to the members of the B.O.O.M. and Merchant laboratories for their aid in this ongoing project. Financial support for this work was provided by the University of Arizona RII Core Facility Pilot Program and NIH grant GM132008

References

1. Ito T, Igarashi H, Jensen RT. Zollinger-Ellison syndrome: recent advances and controversies. Curr Opin Gastroenterol. 2013;29(6):650-661. doi: 10.1097/MOG.0b013e328365efb1

2. Norton, J. A., Foster, D. S., Ito, T., & Jensen, R. T. (2018). Gastrinomas: Medical or Surgical Treatment. In Endocrinology and Metabolism Clinics of North America (Vol. 47, Issue 3, pp. 577–601). W.B. Saunders. https://doi.org/10.1016/j.ecl.2018.04.009

3. Haralick, R. M., Shanmugam, K., & Dinstein, I. (1973). Textural Features for Image Classification. IEEE Transactions on Systems, Man, and Cybernetics, SMC-3(6), 610–621. https://doi.org/10.1109/TSMC.1973.4309314

4. Teo, Y. R., Yong, Y., and Fleming, A. J. (2018) A comparison of scanning methods and the vertical control implications for scanning probe microscopy. Asian Journal of Control, 20: 1352– 1366. https://doi.org/10.1002/asjc.1422.